Egypt. J. Phys. **Vol. 48,** pp. 83-90 (2020)

Egyptian Journal of Physics Science
http://ejfs.journals.ekb.eg/

Development of Advanced, Transparent Radiation Shielding Glass Possessing Boron and Lead Ions in the Glassy Matrix

H. A. Saudi[1*], M. Y. Hassaan[2], E. Tarek[3], E. Borham[4], A. A. Bendary[2]
[1]Physics Department, Faculty of Science, Al-Azhar University (Girls' Branch), Nasr City 11884, Cairo, Egypt.
[2]Physics Department, Faculty of Science, Al-Azhar University, Nasr City 11884,Cairo, Egypt.
[3]Physics Department, Faculty of Science, El-Fayoum University, El-Fayoum, Egypt.
[4]National Centers for Radiation Research and Technology, Egyptian Atomic Energy Authority, Nasr City, Cairo, Egypt.

THE developed shielding glass system x PbO – $10Fe_2O_3$ – (90-x) B_2O_3 (where 25 ≤ x ≤ 45 mol ٪) prepared by melt quenching technique and checked by XRD which reveals the amorphous nature of these glasses. Physical properties were performed by measuring the density at room temperature. Fourier Transform Infrared spectroscopic analysis (FTIR) within the wavenumber range 4000–400 cm^{-1} was carried out to identify the spectral contribution of each component of the structure and results suggests that PbO plays either the role as a modifier or a role of the glass network. The indirect optical energy gaps (E_{opt}) decreased while Urbach energy (E_U) increased with increasing PbO concentration in the studied glass samples. The index of refraction and optical conductivity values are observed to raise with an increasing PbO concentration in the studied glass samples. The results reflected that the increasing of an addition of the values of PbO in Fe_2O_3–B_2O_3 glasses improves the shielding properties. The present glasses possess high mass attenuation for gamma-ray and high mass removal cross-section for the neutrons. Hence, this glass system may be used considered promising to be used in some nuclear applications.

Keywords: Iron Borate Glasses; Molar Volume; Mass Attenuation Coefficient and FTIR Spectroscopy

Introduction

In recent years, the expanding of glass inquires about in the field of shielding is a direct result of their interesting applications with respect to nuclear fields [1–3]. Borate glasses are quite useful as they are commonly easier to be prepared and in addition, they show an enormous different structural unit [4]. It is remarkable that in the borate glasses, B_2O_3 is the essential glass former due to its higher bond strength, lower cation size, smaller heat of fusion [5]. Borate glasses containing heavy metal oxides (HMO) have a special interest because of their remarkable properties and correspondingly their potential stability for certain applications [2]. Especially, the heavy metal oxide glasses containing PbO are optimistic material for their probable applications in the fields of optical communications, laser hosts, X- and γ beams safeguards [3, 6]. Therefore, considerable metal oxide-based glasses are frequently studied because of their high potential in numerous applications [6, 7]. Glasses containing lead ions exhibit high refraction, low dispersion, high electric restriction, a low coefficient of warm extension, and a relatively low melting point. Moreover, Pb ions in glasses, expect a double role either as a glass network former or as a glass modifier. Introducing PbO at the expense of B_2O_3 may change the distribution of B_2O_3in this glass. In the present work, an attempt has been made for the preparation and studying the role of lead oxide in the structural properties and characterization of iron borate glasses. Moreover, to study the shielding properties of gamma-ray and neutron, and the hardness of the prepared glass samples.

*Corresponding author: E-mail: heba_saudi@hotmail.com & heba_saudi@azhar.edu.eg
Received :12/2/2020; accepted :21/4/2020
DOI :10.21608/ejphysics.2020.23900.1035

Also, the optical properties of glass rely upon the nature and the local arrangement of the action the constituent atoms or ions. Additionally, we reported the molar volume, UV and IR spectra of the glass samples.

Experimental Techniques

Glasses with composition x PbO – $10Fe_2O_3$ – (90-x) B_2O_3 glasses (where $25 \leq x \leq 45$ mol %) were prepared by melt quenching technique. Melting was performed in porcelain crucibles set in an electric furnace for around 2 hours at temperature 1100°C.

The density of the glass samples at room temperature was measured by the standard rule of Archimedes utilizing a touchy small scale offset with toluene as inundation fluid (ρ_{liq} =0.866 gm /cm^3 at room temperature). The molar volume V_M of each glass sample was calculated using the formula $V_M = x_i M_i /d$, where x_i is the molar fraction, and M_i is the molecular weight of the i_{th} segment.

The vibration spectra of the glass system were obtained at room temperature utilizing FTIR spectrophotometer model [JASCO FT/IR 300 E (Japan)] in the range 4000–400 cm^{-1}. The measurements were performed directly on glass powder added to the potassium bromide and then pressed to the form of a small disc.

The optical absorption spectra measurements were done in the UV and visible range (from 200 to 1200 nm) with a record twofold shaft spectrophotometer (Type JASCO Corp, V-570, Rel-100, Japan).

Results and Discussion

Density and molar volume

The density measurement is a significant instrument to distinguish the auxiliary changes in the glass network. On the other hand, the molar volume of glass can be ideally used to describe the network structure and the course of action of the structural units, since it manages the spatial structure of the oxygen network. The density measurement and determined molar volume values have shown up in Fig. 1

In the present study, density is observed to increase with the increase of PbO content. This increase might be credited for the change of BO_3 in 4-fold coordinated boron atoms to BO_4 coordination and because of the substitution of low-density boron ions of the high-density by lead ions. Also, non-bridging oxygen decreases in the glass network with increasing PbO content, which will in general, unite their structure, keeping up the homogeneity of the glasses and thus increasing its density [8]. The molar volume demonstrates the spatial distribution of the oxygen in the glass arrange. The observed increment in the molar volume can be credited to the open structure of glasses. The increase in PbO content prompts forming B-O-B linkages with weak covalent B and Pb oxygen bond [8], prompting open structure. This infers Pb enters the glass structure as a farmer of the network. These results will be confirmed in the IR results.

Infrared absorption spectra

Infrared spectrameasurements have been done to recognize the structure of the studied glasses. B_2O_3 could be a basic glass, the units are triangles, which are corner verified in a very random configuration [5]. PbO and FeO enter the glass network each as a network former and additionally as a network modifier and because of this result the structure of this glass is predicted from the previous work of alkali borate glasses [7]. Introducing PbO at the expense of B_2O_3 could be modified the distribution of B_2O_3 in these glasses. The infrared spectra of x PbO-(90-x) B_2O_3-$10Fe_2O_3$ glasses, with x = 25, 30, 35, 40, and 45 mol%, are shown in Fig. 2. The vibrational modes of the borate network are seen to be mainly active in three infrared regions which are similar to those reported earlier [5, 6 and 9]. The group of bands that appeared at 1200–1600 cm^{-1} is because of the asymmetric stretching, relaxation of the B–O band of trigonal BO3 units. The second group of bands lies between 800–1200 cm^{-1} and is because of the B–O bond stretching of the tetrahedral BO_4 units. The third group of absorption bands is observed around 700 cm^{-1} and is because of the bending of B–O–B linkages in the borate network. (The group of bands between 1200-1600 cm^{-1} results from the asymmetric stretching and relaxation of the B–O band of trigonal BO_3 units, the one lieing between 800–1200 cm^{-1} due to the B–O bond stretching of the tetrahedral BO_4 units and the group concerned with absorption bands is observed around 700 cm^{-1} results from the bending of B–O–B linkages in the borate network.) The absorption peak observed in all glass samples in 3204–3217 cm^{-1} is ascribed to hydroxyl or water groups [5] and it is because of the hygroscopic idea of borate glass samples [6]. The peaks around 2270– 2286 cm^{-1} and 2342–2345 cm^{-1} are ascribed to $^{-}$OH group [9]. The absorption peak around 1722–1730 is due to H–O–H bending [5]. The absorption peaks assigned in the IR spectra of the glasses under study are listed in Table 1. From table 1 all of the peaks in the fine spectra are similar except at x = 30%PbO demonstrated the appearance of a peak around 634 cm^{-1}, this is because of B-O-Pb asymmetric bending mode [10] because of Pb atom is heavier than B atom, Pb ion reacts

with boron to produce non bridging oxygen as observed in the sample of x = 45%PbO from the peak around 1265 cm^{-1} that is because of O-Pb-O stretching vibrations [10]. Thus, from Fig. 2 and Table 1, it can be observed that there is no effect of the glass composition on the types of structural groups in the present glass. This might be because of the presence of symmetry $(BO_3)^{3-}$ triangles, BO_4– tetrahedral and asymmetric $(BO_3)^{3-}$ units (i.e. non-bridging oxygen) in each sample [5]. The determined N_4 for the different present glasses is observed to be almost consistent (0.435- 0.469) for various PbO contents as appeared in Fig. 4. (This number exhibits that the glass structure has (short range order) close to the structural units that producing these bands is not influenced by the addition of PbO). The index of refraction is a significant parameter the plan of optical parts, for instance, windows and optical fiber. The values of refractive index for all samples have been estimated from the IR data, by abuse the consequent Sellmeier's relation (1) for room-temperature infrared list of refraction [11,12].

$$n = 1 + \frac{5.58245\,\lambda^2}{\lambda^2 - (0.1625394)^2} + \frac{2.468516\lambda^2}{\lambda^2 - (11.35656)^2} \quad \text{..... (1)}$$

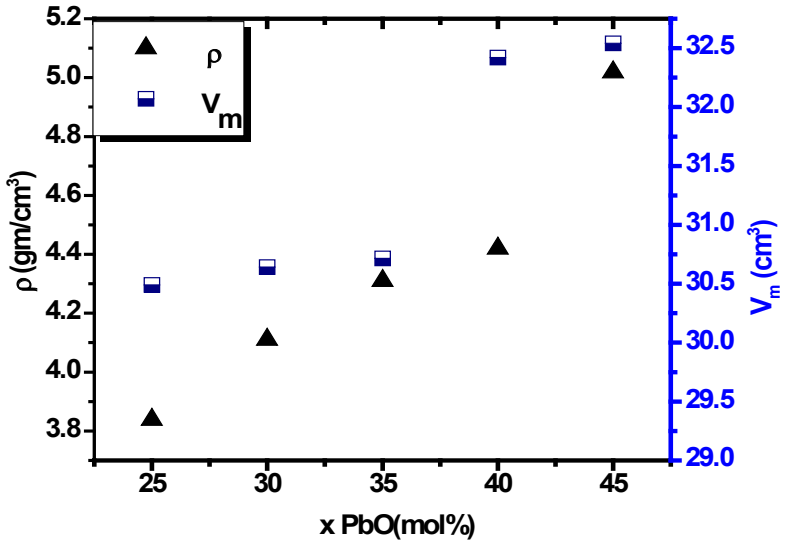

Fig.1. The density and molar volume of different PbO contents in the prepared samples.

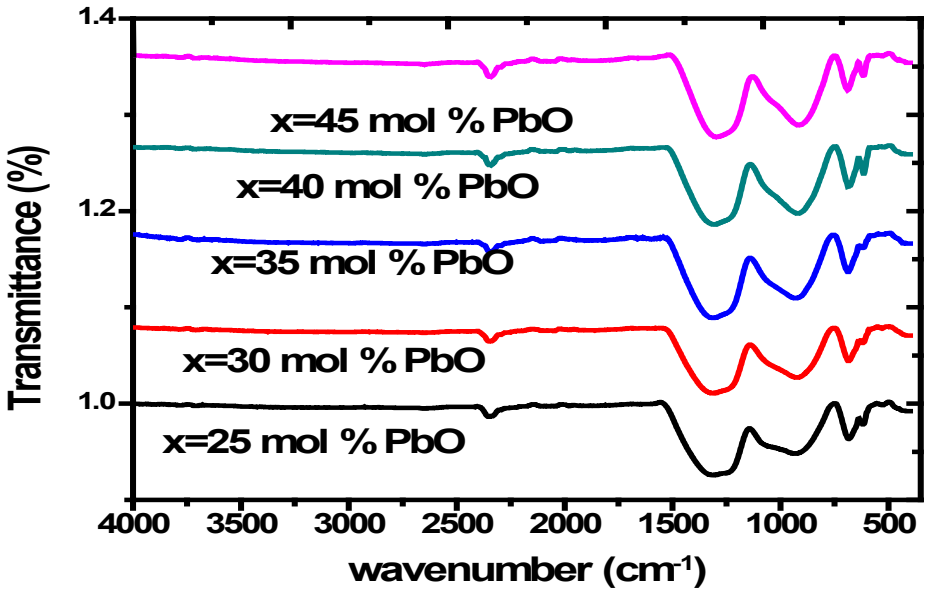

Fig. 2 . FTIR spectra of the glass samples with different contents of PbO

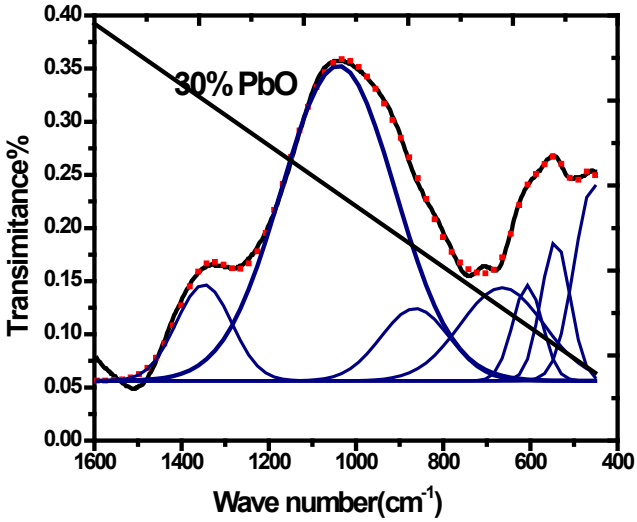

Fig. 3. Example of Deconvlusion of infrared spectrum for glass sample that containing 30% PbO content as a representative sample.

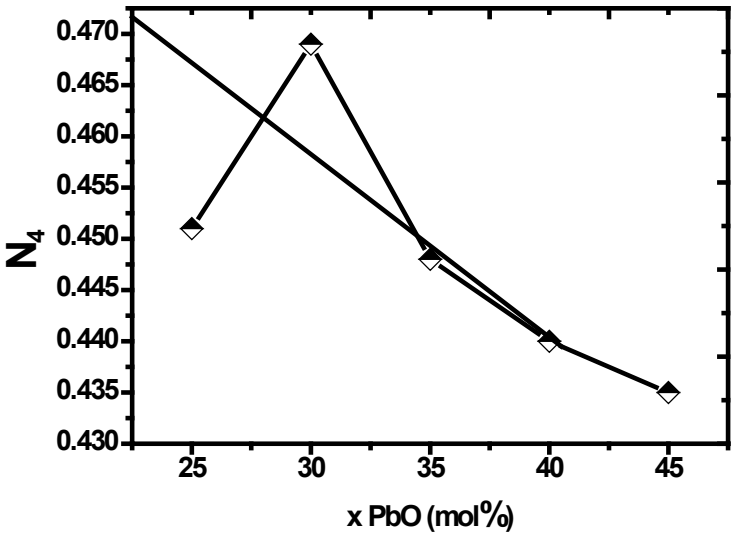

Fig. 4. Dependence of N4 on PbO content.

where λ is the wavelength, for example, one wavenumber of the two observed peaks (950,700 cm^{-1}). The obtained results were recorded in Table 1.

Optical properties

The absorption (*A*) and transmittance (T) of the studied glasses were measured in a wide range of wavelengths as appeared in figures 5, 6 respectively. The analysis of optical spectra is one of the most beneficial tools to figure out the electronic structures of amorphous semiconductors [13]. Measurement of the optical absorption coefficient (α) close to the fundamental absorption edge is especially a standard technique for the examination of optically induced electronic transitions in numerous materials [13].

The absorption coefficient was determined at different wavelengths utilizing the relation:

$$\alpha (U) = 1/d \, (\ln I_o/I) \qquad (2)$$

where (I_0) and (I) are the intensities of the incident and transmitted beams, respectively, and *d* represents the thickness of each sample. Optical band gaps were determined to utilize absorption spectra for indirect transitions for all as prepared glass samples.

TABLE 1. IR peaks and refractive index of the glass system

X (mol%)	Peak position in cm^{-1}	N
25	615, 683, 930, 1314	2.02
30	615, 634, 684, 923, 1314	2.13
35	615, 686, 930, 1314	2.48
40	615, 685, 923,1312	2.79
45	615, 685, 920, 1265	2.94

TABLE 2. Values of Eopt, ΔE, and EF (eV) for the glass samples

X mol% PbO	E_{opt} (eV)	ΔE (eV)	E_F (eV)	Refractive index n	The optical conductivity (σ_{opt}) ($s\ cm^{-1}$)
30	2.59	0.28	3.37	2.1	$1.5*10^{11}$
35	2.81	0.26	3.34	2.4	$2.25*10^{11}$
40	2.96	0.19	3.31	2.7	$3.5*10^{11}$
45	3.06	0.15	3.26	2.9	$5*10^{11}$

$$\alpha(U) = B(hU - E_{opt})^2 / hU \quad (3)$$

Where $n = 2$ for allowing transition, B is a constant and E_{opt} is the indirect optical band gap.

Utilizing the above equations and by plotting $(\alpha hU)^{1/2}$ as a function of photon energy hU. The value of E_{opt} was acquired by extrapolating of $(\alpha hU)^{1/2} = 0$ for indirect transitions [13] has appeared in Fig. 7 as a representative figure. Urbach energy values (ΔE) were calculated by taking the reciprocals of the slope of the linear portion in the lower photon energy region of these curves as stated in equation (4) [14].

$$\alpha(U) = B \exp(hU/\Delta E \quad (4)$$

Table 2 demonstrates the estimations of the indirect band gap and Urbach energies for the prepared glasses. From Table 2 it could be observed that E_{opt} decreases to some degree with increasing PbO contents. The decrease in the band gap hole is a direct result of the development of four coordinated boron units which is affirmed by the band at 920-930 cm^{-1} of IR results that caused a few changes in bonds which are reflected by lowering of band gap values. The decrease in the band gap is also because of the reduction of NBO and the development of bridging oxygen that observed in the IR results. This result also is in accord with results of density measurements about the arrangement of BO_4 units to the detriment of BO_3 units with the increase of PbO content. Additionally, the slight deviation might be because of the role of PbO as a dual network role either modifier or former. The extinction coefficient ($k = \alpha\lambda/4\pi$) could be utilized for Fermi energy (E_F) calculation utilizing Fermi–Dirac distribution function [15]:

$$k(E) = 1/(1 + \exp E - E_F/K_B T) \quad (5)$$

Where k(E) is the maximum absorption at the UV edge, k_B is the Boltzmann constant, E is the incident photon energy, and T is the room temperature (300 K). The E_F values for glass samples are recorded in Table 2, that increased with increasing PbO content. This increase in E_F values might be an immediate result of the increment in acceptor concentration identified with a reduction in donor concentrations, Fermi level can be moved to be adjacent to the conduction band [16]. The refractive index is determined for the prepared glasses based on the optical band gap, according to the following relation [1];

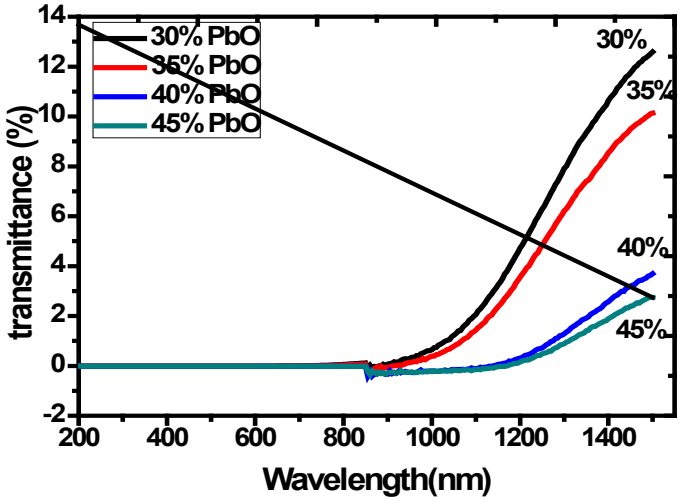

Fig. 5. Optical transmition spectra of the studied glass samples.

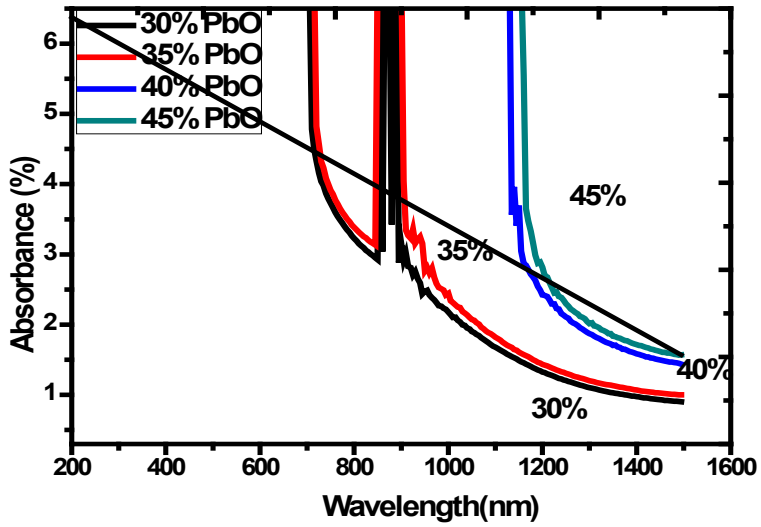

Fig. 6. Optical absorption spectra of the studied glass samples.

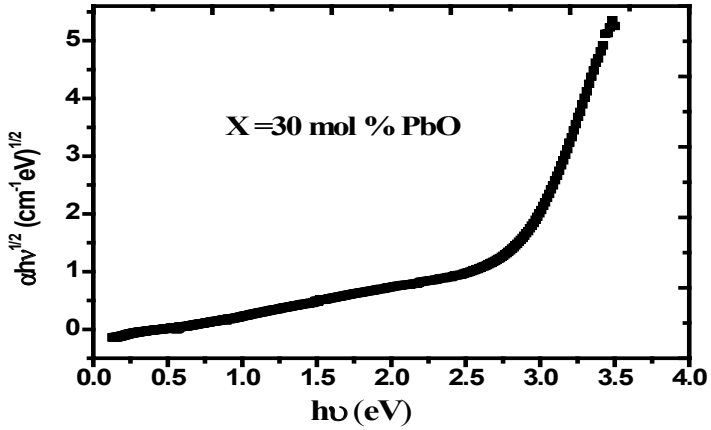

Fig. 7. (αhU)1/2 versus hU for the glass sample of x = 30 mol % PbO as a representative sample.

$$n^2 - 1/ n^2 + 1 = 1 - (E_g /20)^{1/2} \quad (6)$$

The refractive index values demonstrated a continuous increment with increasing of PbO content. The increase in the refractive index (*n)* could be credited to the arrangement of non-bridging oxygen in the glass network and this result agrees with the results of IR. The optical conductivity (σ_{opt}) comes because of the movement of the charge transporters by substituting electric field of the incident electromagnetic waves which are given by the following equation [15];

$$\sigma_{opt} = n\, c\, \alpha / 4\, \pi \quad (7)$$

where n is the refractive index, c is the speed of light in a vacuum, and α is the absorption coefficient. The calculated optical conductivity values appear in table 2. The increase in σ_{opt} with increasing PbO concentration might be a result of the presence of new dimensions in the band gap which facilitate the transition of the electrons from the valence band to these close-by levels, then to the conduction band, thus the band gap decreased, and the optical conductivity increased [15, 17]. Higher values of the optical conductivity reflect the promising utilization of the obtained current from the borate glass doped with PbO in photoelectric devices.

Mass attenuation coefficient of glass samples:

The theoretical estimations of the mass attenuation coefficients (μ_m, cm^2/g) were determined by WinXCom program for the five glass samples at gamma energies 662, 1173, and 1333 keV, and in which photoelectric and Compton scattering interactions are dominating and are given in Fig. 8. It is seen from this figure that the mass attenuation coefficient decreased with increasing gamma energies. The increase of total photon interaction probability at these energies prompts the lessening of gamma-ray transmission with increasing amount PbO. The mass attenuation coefficients were increased with increasing of PbO content in glass matrix demonstrating the better shielding impact. Additionally, estimations of μ_m are reliant on the essential arrangement and thus on the glass density (ρ) [5,7].

The mean free path (λ) of the glass samples

The mean free path λ is the normal separation of a single particle goes through a given material before interacting with other material. From figure 9, λ values of the glass samples were decreased with increasing content of PbO, which additionally was observed in the increase of the mass attenuation coefficient and density results**.**

An effective removal cross section (ΣR) of fast neutron

The removal cross-section (*ΣR*) is the likelihood that a fast, or fission energy, neutron undergoes a first crash, which expels it from the group of penetrating, (uncollided neutrons). If the glass contains enough moderating material, the attenuation of neutrons will be controlled by this removal procedure [5, 11]. An approximate method for calculating the attenuation of fast neutrons using an effective removal cross-section ΣR/ρ ($cm^2\ g^{-1}$) for compounds and homogeneous mixtures by: $\Sigma_R = \sum_i w_i\, (\Sigma_R / \rho)_i$ [11] where w_i is the partial density (g cm^{-3}) and ρ refers to i_{th} constituents' density. The calculated fast neutron effective removal cross-sections (ΣR/ρ) for the glass samples are given in Fig. 8. The calculated values of (ΣR/ρ) demonstrated that, the effective removal cross-section (□R/□) of fast neutrons identifies with the glass density, where 45 PbO (mol%) sample have the smallest value and 25 PbO (mol%) sample have the largest value of (ΣR/ρ), i.e. ΣR/ρ approximately decreases with increasing the glass density, molar volume and the percentage of lead oxide as shown in figure 10. At that point, it is presumed that the elemental composition, lead % and the glass density contributes an important rule for neutrons and gamma-rays attenuation. Also, from IR results, it was found that the existence of iron and lead oxides as glass modifiers help to absorption of neutron energy. Therefore, the lack of removal section with increased lead content, the minimum concentration of lead is (25 mol%) was found better than other glasses in other previous researches [1, 5 and7]. And therefore, less glass thickness requires is to be utilized as a protective shield of neutrons, So, lead borate glass is used for gamma rays shielding with a high concentration of lead while for neutrons low concentration of lead could be utilized for the studied samples. The glass density just as the boron and lead content must be taken into consideration.

Conclusion

The density of the glass samples increments gradually with the increase of PbO content. The molar volume appears to increase due to the open structure of glasses so Pb, Fe act almost as a modifier in the glass network. The groups like BO_3 and BO_4 act as network structural groups while FeO_6 and PbO appeared in interstitial positions. The studied glass systems obey the Urbach rule due to the dependence of the absorption coefficient (α) on photon energy and the indirect band gaps. The value of the width of the tails of localized states (ΔE) varied between 0.28 and 0.15 eV depending on the PbO content. The results obtained from the density, FTIR spectroscopy, and band gap energy measurements agree with each other. The results of gamma-ray and neutron shielding reveal properties that the glasses in this work were better as radiation shielding materials in term of their volume required for shield design and with the advantage of being transparent to visible light. The Compton scattering gives a dominant contribution to the total mass attenuation coefficients for all the studied glass samples.

Compliance with ethical standards

Conflict of interest The authors declare that they have no competing interests.

Conflict of interest

The authors declare that they have no conflict interest.

Reference

1- Aly Saeed, Y. H. Elbashar, S. U. El Khameesy, *Silicon,* 10, 569-574, (2018). DOI 10.1007/s12633-016-9492-y

2- Rayan DA, Elbashar Y, Rashad MM, El-Korashy A, *J. Non-Cryst Solids* 382 (15): 52–56, (2013).

3- Elhaes H, Attallah M, Elbashar Y, Ibrahim M, El-Okr M, *J Phys B: Condens Matter* 449(15):251–254, (2014).

4- D. L. Griscon, "Electron Spin Resonance," *Glass Science and Technology,* Vol. 48, 151-251 (1990).

5- H. A. Saudi, A. G. Mostafa, N. Sheta, S.U. ElKameesy and H. A. Sallam, Physica B: Physics of Condensed Matter 406, 4001-4006, (2011).

6- D. L. Griscon, "Materials Science Research—Borate Glasses 12," Plenum Press, New York, 1978.

7- H. A. Saudi, H. A. Sallam, K. Abdullah, *Physics and Materials Chemistry,* Vol. 2, No. 1, 20-24, (2014).

8- A. Chahine, M. Et-tabirou and J. L. Pascal, *Materials Letters,* Vol. 58, No. 22-23, 2004, pp. 2776- 2780. doi:10.1016/j.matlet.2004.04.010.

9- Hiroyo Segawa, Naoto Hirosaki, Ceramics International, Vol. 44, Issue, 4783-4788 (2018).

10- M. Rafiqul Ahsan, M. Alfaz Uddin and M. Golam Mortuza, *Indian J. of Pure and Applied Physics,* Vol.43, pp. 89-99 (2005).

11- Wallace D.Fragoso, Celso de Mello Donega and Ricardo L.Longo, *J. Non-Crystalline Solids* 351 (2005).

12- H. A. Saudi, H. M. Gomaa, Radiation Detection Technology and Methods 3 (1), 7 (2019).

13- Vandana Sharma1 et al, *New Journal of Glass and Ceramics*, 2, 128-132 (2012).

14- P T DESHMUKH, D K BURGHATE, V S DEOGAONKAR, S P YAWALE and S V PAKADE, *Bull. Mater. Sci.,* Vol. 26, No. 6, pp. 639–642 (2003). © Indian Academy of Sciences.

15- T. A. Taha, A. S. Abouhaswa, *Journal of Materials Science: Materials in Electronics,* 29, P.8100–8106 (2018).

16- F. El-Diasty, M. Abdel-Baki, F.A. Abdel-Wahab, *Opt. Quant. Electron,* **48** (4), 273 (2016).